

JAAS

Accepted Manuscript



This is an *Accepted Manuscript*, which has been through the Royal Society of Chemistry peer review process and has been accepted for publication.

Accepted Manuscripts are published online shortly after acceptance, before technical editing, formatting and proof reading. Using this free service, authors can make their results available to the community, in citable form, before we publish the edited article. We will replace this *Accepted Manuscript* with the edited and formatted *Advance Article* as soon as it is available.

You can find more information about *Accepted Manuscripts* in the [Information for Authors](#).

Please note that technical editing may introduce minor changes to the text and/or graphics, which may alter content. The journal's standard [Terms & Conditions](#) and the [Ethical guidelines](#) still apply. In no event shall the Royal Society of Chemistry be held responsible for any errors or omissions in this *Accepted Manuscript* or any consequences arising from the use of any information it contains.

On-line separation and preconcentration of hexavalent chromium on a novel mesoporous silica adsorbent with determination by solution-cathode glow discharge-atomic emission spectrometry

Jiaxian Ma ^{a,b}, Zheng Wang ^{*a}, Qing Li^a, Rongyin Gai^a, Xiaohong Li^a

^aShanghai Institute of Ceramics, Chinese Academy of Science, Shanghai, 200050, China. E-mail: wangzheng@mail.sic.ac.cn; Fax: (+86)21-52413016; Tel: 86-21-52413503; Address: 1295 Dingxi Road, Shanghai, 200050 P. R. China.

^bSchool of Materials Science and Engineering, Shanghai University, Shanghai 200072

Abstract:

A flow injection (FI)-technique based on an on-line solid phase extraction (SPE) separation system coupled with solution-cathode glow discharge-atomic emission spectrometry (SCGD-AES) detection was developed for the determination of hexavalent chromium in aqueous samples. In this system, Cr(VI) was separated and preconcentrated on a novel lysine-modified mesoporous silica (Fmoc-SBA-15) at pH 5, and detected after elution. An enrichment factor of 91 was achieved under optimized experimental conditions, at a FI flow rate of 1.5 mL·min⁻¹ and 0.1 mol·L⁻¹ NH₃·H₂O for Cr(VI) elution. A FI-SCGD-AES detection limit of 0.75 µg·L⁻¹ could be achieved, with a linear range of 10–10000 µg·L⁻¹. The precision of nine replicate Cr(VI) measurements was 4.2% at 100 µg·L⁻¹. The accuracy was validated using a certified reference material of riverine water (GBW08607).

Keywords: Mesoporous material; Cr(VI); SPE; Solution-cathode glow discharge.

Introduction

Chromium pollutants are discharged by various industries such as electroplating, leather tanning, mining, steel making, and pigments, and chromium exposure has a significant impact on the health of humans as well as other living organisms.¹⁻⁴ In solution, chromium is usually found in the Cr (VI) and Cr (III) oxidation states. Cr (III) is an essential element for biological mechanisms, controlling glucose, lipid, and protein metabolism. Conversely, Cr (VI)-containing compounds are highly toxic materials and Cr (VI) is soluble in water over nearly the entire pH range⁵. The United State Environmental Protection Agency (EPA) has regulated the permissible limit of 100 µg·L⁻¹ of total chromium in drinking water. In 2014, some states in USA (like California) have new regulations with less than the allowable levels set by EPA. In China and Japan, the maximum allowable concentration of Cr (VI) in wastewater is 100 µg·L⁻¹ and 50 µg·L⁻¹, respectively.

1
2
3 However, World Health Organization thought that the guideline value of $50 \mu\text{g}\cdot\text{L}^{-1}$ of Cr (VI) was
4 too high, compared with its high risk of carcinogenicity. Consequently, the development of fast,
5 sensitive, and reliable analytical methods, as well as the speciation method of chromium, in
6 environment is absolutely required.
7
8

9
10 Under usual conditions, the speciation of chromium is carried out by combining selective
11 separation and/or preconcentration procedures with sensitive detection techniques. Several
12 analytical methods—including an on-line solid-phase extraction (SPE) separation system with
13 flame atomic absorption spectrometry (FAAS)^{6–12} and electrothermal atomic absorption
14 spectrometry (ETAAS),^{13–17} and high performance liquid chromatography (HPLC) with
15 inductively coupled plasma–mass spectrometry (ICP–MS)^{18–20} have been developed for the
16 quantitative determination of chromium species in aqueous solutions. These methods have many
17 attractive features: low detection limits, wide linearity, and good precision. However, they also
18 suffer several shortcomings, often requiring high power and inert or special gases, and operation at
19 high temperature and even under high vacuum.
20
21

22
23 In recent years, an ambient microplasma source known as solution-cathode glow discharge
24 (SCGD, also named ELCAD, electrolyte cathode discharge) has emerged as an important tool in
25 atomic spectrum analysis.^{21–27} It is now regarded as one of the most promising alternative
26 miniaturized excitation sources due to the low detection limits (DLs) achievable for many metals,
27 low power consumption (~ 75 W), lower construction/operating costs, and no need vacuum. The
28 discharge, coupled with atomic emission spectrometry (SCGD-AES), has been successfully
29 applied in the quantitation of trace metal ions in different samples.^{28–30} In recent studies,
30 SCGD-AES has provided DLs for many metals at or below the tens of parts per billion
31 range.^{26,27,30,31}
32
33

34
35 Unfortunately, recent studies demonstrate that SCGD-AES cannot meet the demand for the
36 determination of Cr at very low levels in complex samples. The DLs for Cr were only 900, 200 and
37 $76 \mu\text{g}\cdot\text{L}^{-1}$ in preliminary studies.^{32,33,34} To lower the DL for Cr, organic compounds such as
38 HCOOH ³⁴ and CTAC (cetyltrimethylammonium chloride)³⁵ have been used to improve the
39 emission signals. It was reported that 20% (v/v) HCOOH enhanced the sensitivity of ELCAD-AES
40 for the analytes, improving the DL of Cr to $65 \mu\text{g}\cdot\text{L}^{-1}$.³⁴ Additionally, the net intensity of the
41 atomic emission lines of Cr solutions with 0.15% (mass percentage) CTAC improved by 2.6-fold,
42 compared with solutions without CTAC, affording DL of Cr for $42 \mu\text{g}\cdot\text{L}^{-1}$.³⁵ However, the DLs
43 were still much higher than those from other detection systems such as ETAAS and ICP-MS, and
44 far from levels normally required.
45
46

47
48 Separation and preconcentration are good techniques for increasing the determination ability of Cr
49 and eliminating matrix interference. Separation methods reported in the literature are usually based
50 on coprecipitation,^{36,37} solvent extraction,³⁸ ion exchange,^{39,40} HPLC,^{18–20} and solid phase
51 extraction.^{6–17} Among these methods, SPE has become a very powerful and efficient sample
52
53
54
55
56
57
58
59
60

pretreatment method. In a successful SPE procedure, a key factor is the identification of an appropriate adsorbent. Mesoporous silicas are widely used in adsorption applications due to their selectivity, stable mesoporous support structure, and good dispersibility in aqueous solutions. In a previous study, considering that adsorbents possessing N-containing functional groups (such as 3-aminopropyltriethoxysilane, imidazole, triazole, and 2-mercaptopyridine) effectively formed complexes with chromium ions,^{6,41-44} an amine-modified mesoporous material was employed in SPE for the selective retention of inorganic Cr(VI) complexes. Nevertheless, the Cr(VI) adsorption capacity of the material was limited, which could result in a low EF.

Here, a novel lysine-modified mesoporous material was synthesized to introduce additional amino groups. The material was packed in a discoid microcolumn for SPE to increase the sensitivity of SCGD-AES for Cr(VI) determination and separate Cr(III) using flow injection (FI) techniques coupled with SCGD-AES. To the best of our knowledge, no such studies have been reported so far. The effects of the solution flow rate, presence of other ions, EF, and the eluent were investigated. Finally, the method was validated against a certified reference material (GBW08607).

Experimental Section

Reagents and materials

Doubly deionized water (DIW, 18.25 M Ω -cm) obtained from a Milli-Q water system (Millipore, Bedford, MA, USA) was used throughout the experiment. The reagents listed below were of analytical grade or better. The (3-aminopropyl)triethoxysilane (APTES) were obtained from Sigma-Aldrich. *N*- α -Fmoc-*N*- ϵ -Boc-L-lysine (99%, M_{av} = 468), H₂O₂, HCl, and NH₃·H₂O solutions, and tetraethyl orthosilicate (TEOS) were obtained from Shanghai Sinopharm Chemical Reagent Co., Ltd., China. HNO₃ (65%, ACS reagent) was obtained from Sigma-Aldrich. Dicyclohexylcarbodiimide (DCC) and 4-dimethylaminopyridine (DMAP) were obtained from Shanghai Medpep Co., Ltd., China.

Organic solvents such as toluene, pyridine, trifluoroacetic acid (TFA), dichloromethane (DCM), ethanol, and dimethylformamide (DMF) (Shanghai Sinopharm) were dried with activated 4Å-type molecular sieves overnight before use. A 1000 $\mu\text{g}\cdot\text{mL}^{-1}$ stock standard solution of Cr (III) was prepared by dissolving chromium (III) chloride hexahydrate in 0.01 mol·L⁻¹ HNO₃, whereas a 1000 $\mu\text{g}\cdot\text{mL}^{-1}$ Cr (VI) solution was obtained by dissolving potassium dichromate in 0.01 mol·L⁻¹ HNO₃. The standard solutions were prepared by dilution of stock standard solutions. The certified reference material GBW08607 (Trace Elements in Water, total concentration of chromium: 0.520 \pm 0.010 $\mu\text{g}\cdot\text{mL}^{-1}$) was obtained from the National Research Center for Certified Reference Materials (Beijing, China). A wastewater sample was obtained from the factory of the East China University of Science and Technology (Shanghai, China), filtered through a 0.22 μm membrane, and adjusted to pH 5.0 with diluted HNO₃. Glassware was soaked in (1 + 1) HCl overnight and cleaned with Milli-Q water before use.

Preparation and characterization of lysine-functionalized mesoporous SBA-15

Lysine-functionalized mesoporous SBA-15 material was synthesized by an easy two-step post-grafting process. In the first step, SBA-15 was treated with APTES in toluene to produce NH₂-SBA-15. Then, the lysine-grafted mesoporous silica was synthesized by reaction between NH₂-SBA-15 and *N*- α -Fmoc-*N*- ϵ -Boc-L-lysine. The NH₂-SBA-15 (~1 g), *N*- α -Fmoc-*N*- ϵ -Boc-L-lysine (6 g), DCC (3.08 g), and DMAP (0.05 g) were added to DMF (200 mL). The mixture was heated at 80 °C for 24 h under nitrogen atmosphere. The resulting solid was filtered, washed sequentially with DMF, ethanol, and water, and then dried in air atmosphere at 80°C for 5 h. This sample was named lysine-SBA-15.

To remove the hydrophobic *t*-butyloxycarbonyl (Boc) group, lysine-SBA-15 (0.5 g) was dissolved in dichloromethane (16 mL) and trifluoroacetic acid (4 mL) with stirring for 2 h at room temperature. The resulting solids were filtered, washed successively with deionized water and ethanol, and dried in air atmosphere at 80°C for 5 h. **Scheme 1** shows the synthetic route for Fmoc-SBA-15.

Instrumentation

A schematic diagram of the new FI-SCGD-AES system can be found in **Figure 1**. A detailed description of the instrument components follows.

SCGD Cell Design and Emission Optics

An illustration of the new cell design can be found in **Figure.1**. The improved SCGD cell was designed to enhance portability as compared to the previous SCGD configuration.²¹ In particular, a glass capillary (internal diameter, 0.38 mm; external diameter, 1.1 mm) was directly connected to the graphite rod by insertion through a hole on one side of the graphite rod to remove the influence of the constant solution level. The graphite rod passes horizontally through a hole drilled in one wall of the reservoir. This arrangement is similar to the design proposed by Shekhar²⁸ and Doroski³¹, but we retained the reservoir as a fixed device.

A Kepco (Flushing, NY) BHK 2000-0.1MG high-voltage power supply was used in constant voltage mode. To limit the discharge current, a 1.2 k Ω ballast resistor was introduced in series with the anode. A peristaltic pump (Gilson, France) with two channels was used to pump sample solutions and carry waste solutions from the overflow reservoir. The sample solution was pumped into the SCGD cell through the glass capillary. Positioned 3 mm above the capillary tip was a tungsten rod that served as the anode for the cell. The tip of the rod closest to the micropipette was tapered (tip angle of 45°) to create a pointed structure that resulted in a more stable discharge. The waste was discharged steadily from the glass pipette (i.d. = 2.8 mm, o.d. = 4.4 mm). The discharge was imaged at a magnification of 2.3:1 by a quartz lens positioned on the vertical entrance slit of a monochromator (Princeton Instruments, Action SP 2500, USA) equipped with a photomultiplier

1
2
3 biased at 700 V that was used as the detector. Emission spectra were recorded with an integration
4 time of 0.5 s at 0.05 nm intervals. SpectraSense (Princeton Instruments) version 4.4.6 software was
5 used to operate the spectrometer, control its configuration, and collect and process the data.
6
7

8 9 **On-line solid-phase extraction**

10
11 The FI system consisted of a flow injection analysis instrument (FIA-3110, Beijing Titan
12 Instruments, China) and a discoid packed column (o.d. = 3 cm, i.d. = 0.22 μm). Effluent from the
13 on-line solid-phase extraction system was directed into the sample capillary. The two peristaltic
14 pumps of the FI system were active during the whole operation process. The FI-SCGD-AES
15 operating program is presented in **Table 1**. To adjust the concentration of the eluent to pH 1 before
16 flowing into the SCGD-AES, an additional solution consisting of 7% HNO_3 was injected.
17
18
19

20 21 *Apparatus*

22
23 Powder XRD patterns were collected on a Rigaku D/Max 2200 PC diffractometer (Rigaku
24 Corporation, Japan) using $\text{Cu K}\alpha$ radiation at 40 kV and 40 mA. Transmission electron microscopy
25 (TEM) images were recorded on a JEOL 200 CX electron microscope (JEOL, Japan) at 160 kV.
26 The IR spectra were collected using a Nicolet 6700 FTIR spectrometer. The pH was measured
27 using a PHS-3E digital pH meter (Shanghai Precision and Scientific Instrument, China). The
28 solutions were measured by FI-SCGD-AES and inductively coupled plasma-atomic emission
29 spectroscopy (ICP-AES) (Varian Vista AX, America). The wavelength used for the SCGD
30 determination of Cr was 357.9 nm.
31
32
33
34

35 36 **Results and discussion**

37 38 *Characterization of sorbent*

39
40 The small angle XRD pattern of SBA-15 shows one intense peak at (100) and two small,
41 well-resolved peaks at (110) and (200), describing the well-ordered 2D hexagonal structural
42 symmetry that is typical for the highly ordered SBA-15 mesoporous structure. The
43 Fmoc-SBA-15 pattern shows only the intense peak at (100), which indicates that the ordering of
44 the mesoporous structure decreased with the introduction of the functional groups. The intensities
45 of the XRD peaks for Fmoc-SBA-15 are slightly lower than those measured for SBA-15, which
46 provides evidence that the functionalization primarily occurred inside the mesopore channels.
47 The functionalization is probably caused by the pore filling effect of the SBA-15 channels or by
48 the anchoring ligands on the surface of SBA-15.^{45,46} The TEM images of the Fmoc-SBA-15
49 sample, obtained with the electron beams parallel and perpendicular to the pore channels, are
50 shown in **Figure 2**. These findings are consistent with the XRD results, indicating that the
51 modified materials maintained their well-ordered mesoporous structure after grafting.
52
53
54
55
56
57
58
59
60

1
2
3 FT-IR was used to confirm the presence of APTES and lysine in the silicate framework. The
4 characteristic peaks around 1250–1000 and 3400 cm^{-1} were attributed to the Si–O–Si and –OH
5 stretching vibrations, respectively. The stretching bands at 2870 and 2938 cm^{-1} were attributed to
6 the asymmetric and symmetric C–H stretching in the aliphatic chains of the aminopropyl groups
7 and the lysine in Fmoc-SBA-15. The band at about 1560 cm^{-1} can probably be attributed to NH_2
8 bending, which was especially intense for Fmoc-SBA-15, indicating the presence of amino groups.
9 The intense band at about 1679 cm^{-1} in the Fmoc-SBA-15 spectrum was attributed to the amide
10 $\text{C}=\text{O}$,⁴⁷ which provides important evidence for the presence of lysine. These results confirmed that
11 SBA-15 was successfully functionalized with lysine.
12
13
14
15

16 17 *The effect of pH on Cr adsorption*

18
19 The solution pH is one of the key factors that may affect the distribution of the Cr species, the
20 adsorption performance, and the adsorbent surface properties.⁴⁸⁻⁵¹ To investigate the effect of
21 solution pH on the adsorption capacity of Fmoc-SBA-15, a set of adsorption experiments was
22 performed using about 10 $\text{mg}\cdot\text{L}^{-1}$ Cr (VI) and Cr (III), 1 $\text{g}\cdot\text{L}^{-1}$ adsorbent dose within the range pH
23 1–9 by HNO_3 and $\text{NH}_3\cdot\text{H}_2\text{O}$ solutions.
24
25
26

27 The effect of pH on the Cr (VI) and Cr (III) uptake is shown in **Figure 3**. In the tested pH range, the
28 Cr (VI) adsorption rate was relatively high, whereas Cr (III) exhibited almost no adsorption.
29 Thus, the lysine-modified material has great potential for the separation of Cr (VI) and Cr (III).
30 Below pH 3, Cr (VI) adsorption sharply decreased with the decrease of pH, a plateau was achieved
31 within pH 3-7, whereas at pH higher than 7, Cr (VI) adsorption decreased with increasing pH. This
32 can be explained in this way: Cr (VI) can exist in aqueous solution in different ionic forms
33 (HCrO_4^- , CrO_4^{2-} , $\text{Cr}_2\text{O}_7^{2-}$), which depend on solution pH. At $\text{pH} < 3$, Cr (VI) was existing as
34 neutral acid, its electrostatic interaction with the protonated amino-groups was negligible, and
35 thus its absorption was not favorable. At pH 3-7, HCrO_4^- and $\text{Cr}_2\text{O}_7^{2-}$ are the principal forms,
36 indicating a maximum electrostatic interaction between Cr (VI) and the protonated amino-groups,
37 which corresponded to a maximum absorption. When $\text{pH} > 7$, the predominant form of Cr (VI) is
38 $\text{Cr}_2\text{O}_7^{2-}$. It is obvious that the dimensions of a $\text{Cr}_2\text{O}_7^{2-}$ ion are about twice those of an HCrO_4^- ion.
39 This larger size would reduce the ability of a $\text{Cr}_2\text{O}_7^{2-}$ ion to enter the pores of the mesoporous
40 silica, resulting in the lower adsorption capacity. Thus, pH 5 was selected for further studies herein.
41 The maximum Cr (VI) adsorption capacity of Fmoc-SBA-15 was 76 $\text{mg}\cdot\text{g}^{-1}$ and it could reach Cr
42 (VI) adsorption equilibrium with 30 mg Fmoc-SBA-15 in the first 2 min.
43
44
45
46
47
48
49

50 51 *Optimization of SCGD-AES*

52
53 The analytical characterization of the proposed method was conducted under preliminary
54 conditions (an empty discoid packed column, electrode gap of 3 mm, slit width of 50 μm , and
55 integration time of 0.5 s). Light emitted from the SCGD was collected from 0.6 mm diameter spot
56 within the negative glow positioned 1 mm above the top of the center of the capillary. A
57
58
59
60

1
2
3 background emission spectrum of the $0.1 \text{ mol}\cdot\text{L}^{-1}$ HNO_3 solution by the SCGD was obtained,
4 which was similar to most other solution-electrode discharges.³⁵
5
6

7 Based on the initial study, a $10.0 \text{ mg}\cdot\text{L}^{-1}$ solution of Cr(VI) and an aqueous blank adjusted to pH
8 1.0 with HNO_3 were chosen as model analytes to further investigate the characteristics of the
9 SCGD system. To optimize emission signals and DLs, the effects of voltage (from 1030 to 1090 V)
10 and sample introduction flow rate (from $1.5 \text{ mL}\cdot\text{min}^{-1}$ to $2.0 \text{ mL}\cdot\text{min}^{-1}$) were evaluated. Eleven
11 continuous measurements of emission signals were collected at the appropriate wavelength for Cr
12 (VI) (357.9 nm) from a blank solution for calculation. The DL was calculated using the definition
13 $\text{DL} = 3s\cdot k^{-1}$, where s is the standard deviation corresponding to the 11 continuous measurements of
14 the blank samples and k is the slope of the calibration curve. Multiple readings ($n = 7$) for each Cr
15 (VI) solution and the acid blank solution were recorded. For optimization studies, the minimum
16 DLs were designated as the analytical parameter to be evaluated. The optimized DL was calculated
17 to be $68 \text{ }\mu\text{g}\cdot\text{L}^{-1}$ for Cr(VI) at an applied potential of 1100 V (with a corresponding current of 71
18 mA and power of 78.1 W) and flow rate of $2.0 \text{ mL}\cdot\text{min}^{-1}$.
19
20
21
22
23
24

25 *Optimization of FI*

26
27 To achieve the optimal conditions for the separation and pre-concentration of Cr (VI), the amount
28 of mesoporous material, flow rate, and eluent were studied.
29
30

31 **Figure 4** shows the effect of the amount of mesoporous material on the adsorption rate of Cr (VI).
32 To obtain an optimal adsorption rate, different amounts of Fmoc-SBA-15 (5, 10, 15, 25, 30, 35, and
33 40 mg) were added to the discoid microcolumn, and then $1.0 \text{ mg}\cdot\text{L}^{-1}$ Cr (VI) solution (5 mL) was
34 passed through the microcolumn at a flow rate of $2.0 \text{ mL}\cdot\text{min}^{-1}$. The adsorption rate increased
35 enormously from 62 to 98% in the range of 5 to 30 mg due to the increase of touch opportunity
36 between materials and sample solution. The adsorption decreased slightly (by 10%) when 40 mg
37 material was used because the higher pressure forced the sample solution to exit the microcolumn
38 without touching the material. Thus, 30 mg was selected as the optimal material amount.
39
40
41
42

43 The effect of the sample flow rate on Cr(VI) retention was investigated by passing 1.0 and 10.0
44 $\text{mg}\cdot\text{L}^{-1}$ Cr(VI) solutions (5 mL each) through the discoid microcolumn packed with 30 mg
45 mesoporous material, at flow rates ranging from 1.0 to $5.0 \text{ mL}\cdot\text{min}^{-1}$. In addition, $0.1 \text{ mol}\cdot\text{L}^{-1}$
46 $\text{NH}_3\cdot\text{H}_2\text{O}$ (5 mL) was chosen as eluent at a flow rate of $2.0 \text{ mL}\cdot\text{min}^{-1}$. A 97% adsorption ratio was
47 exhibited over the wide range of flow rates. To achieve rapid analysis, it is necessary to choose a
48 high flow rate, but the pressure of the discoid microcolumn increases with increasing flow rate.
49 When the flow rate was over $5.0 \text{ mL}\cdot\text{min}^{-1}$, sample leakage occurred. Here, $4.0 \text{ mL}\cdot\text{min}^{-1}$ was
50 selected as the optimal flow rate.
51
52
53
54

55 Different concentrations of $\text{NH}_3\cdot\text{H}_2\text{O}$ were investigated to identify the optimal desorption agent
56 amount, ranging from 1 to $0.001 \text{ mol}\cdot\text{L}^{-1}$ aqueous $\text{NH}_3\cdot\text{H}_2\text{O}$. The desorption ratios of Cr (VI) ions
57 were very high (up to 99%) in the range $0.01\text{--}1 \text{ mol}\cdot\text{L}^{-1}$ $\text{NH}_3\cdot\text{H}_2\text{O}$. In addition, the elution speed in
58
59
60

0.01 mol·L⁻¹ NH₃·H₂O was lower than in 0.1 and 1 mol·L⁻¹ NH₃·H₂O. Given the above considerations, 0.1 mol·L⁻¹ NH₃·H₂O was selected for further studies. However, the plasma in our SCGD device could not be kept stable in alkaline solution. In this study, the acidity of the injection solution containing 0.1 mol·L⁻¹ NH₃·H₂O was much less than pH 1, which might have changed the resistance of the solution and resulted in current and intensity changes. The use of additional solution was a practical way to meet the acidity demands of our SCGD.

Additional solutions of 6, 6.5, 7, 7.5, and 8% (v/v) HNO₃ were injected in the SCGD at a flow rate of 0.5 mL·min⁻¹. The SCGD-AES injection rate was maintained at 2.0 mL·min⁻¹, which led to a 4/3 dilution of the concentration of Cr (VI) eluted from the material. The experiment result showed that the pH of solution which entered the SCGD was about 1.0 and the plasma was stable when adding 7% HNO₃.

Coexisting ion interference

The effects of other anions and cations on the pre-concentration and determination of Cr (VI) were investigated under the optimal conditions described above; the results are shown in **Table 2**. The tests were carried out at a fixed Cr(VI) concentration of 100 µg·L⁻¹, with interference from the representative alkaline and alkaline earth metal ions Na(I), Mg(II), and Ca(II), the transition metal ions Cu(II), Zn(II), and Cr(III), other metal ions such as Al(III) and Pb(II), and the anions SO₄²⁻, NO₃⁻, Cl⁻, and H₂(PO₄)⁻.

As shown in **Table 2**, the results indicate that changes in Cr (VI) preconcentration and determination were observed in the presence of 1000 µg·L⁻¹ Pb (II), 5000 µg·L⁻¹ Ca (II) and Zn (II), 500 µg·L⁻¹ Cr (III), 4000 µg·L⁻¹ Mg (II) and Al (III), 20000 µg·L⁻¹ SO₄²⁻, 50000 µg·L⁻¹ NO₃⁻ and Cl⁻, and 100000 µg·L⁻¹ H₂(PO₄)⁻. The analytical recoveries were all above 86%.

Analytical figures of merits

Under optimized experimental conditions, at a FI flow rate of 1.5 mL·min⁻¹ and 0.1 mol·L⁻¹ NH₃·H₂O for Cr(VI) elution, an enrichment factor of was found to be 91, which is defined as the slope ratio of the calibration curves for the determination of Cr by SPE-SCGD-AES and single SCGD-AES, respectively. The high EF is due to three amino-groups in the new material compared to the original NH₂-SBA-15⁶ material which is only one. According to the IUPAC definition, the limits of detection were calculated as the concentration of analyte yielding a signal equivalent to three times of the standard deviation of the blank value (n=7). A FI-SCGD-AES limits of detection of 0.75 µg·L⁻¹ could be achieved, and the linear concentration range of the calibration curve was 10–10000 µg·L⁻¹ with a correlation coefficient of 0.9997. The precision of nine replicate Cr (VI) measurements was 4.2% (RSD) at 100 µg·L⁻¹.

The analytical performance of the SPE-SCGD-AES for the determination of Cr is listed in **Table 3**, and is compared with recent literature related to SCGD-AES or ELCAD-AES. The DL of Cr in the

1
2
3 present work is significantly better than those in the recent studies, and is improved more than
4 50-fold compared to the best reported Cr DL value by SCGD-AES ($42 \mu\text{g}\cdot\text{L}^{-1}$)³⁵. A comparison of
5 the present method with other methods for Cr (VI) determination is shown in **Table 4**. The
6 proposed method exhibited a higher EF (91) and a wider linear range than almost all of the other
7 reported techniques. On the other hand, the SCGD-AES that we used here was much cheaper than
8 most of these detection techniques. It is likely to be used for detection in the field because it can be
9 operated without any special gases or vacuum equipment.
10
11
12
13

14 15 16 *Validation and applications* 17

18
19 The developed method was applied in the analysis of Cr (VI) and Cr (III) in DIW and wastewater
20 samples. The results are presented in **Table 5**. Cr(VI) determination was carried out using 0.1
21 $\text{mol}\cdot\text{mL}^{-1}$ $\text{NH}_3\cdot\text{H}_2\text{O}$ as the eluent, and Cr(III) was converted to Cr(VI) for total chromium analysis,
22 after which Cr(III) was finally obtained by subtraction. For DIW, Cr (III) and Cr (VI) have not
23 been determined. When $50.0 \mu\text{g}\cdot\text{L}^{-1}$ Cr (VI) was added to the sample, the determination result was
24 $51.2 \pm 1.6 \mu\text{g}\cdot\text{L}^{-1}$ and the Cr (VI) recovery was 102 %; this indicated excellent Cr (VI) recovery
25 from the solution. Similar results were obtained in wastewater (the wastewater composition
26 included a high concentration matrix of Ca, Mg, Na, SO_4^{2-} , and K, among other ions). Under the
27 aforementioned conditions, the method was validated by determining the total Cr content in the
28 certified reference material GBW08607. The Cr concentration was determined as 0.520 ± 0.010
29 $\mu\text{g}\cdot\text{mL}^{-1}$. Cr (III) was then oxidized to form Cr (VI) by treatment with hydrogen peroxide in
30 NaOH. The total concentration of Cr(VI) was determined as $0.523\pm 0.004 \mu\text{g}\cdot\text{mL}^{-1}$, which is in
31 good agreement with the certified values reported by Wang⁶ and Huang.⁵³ Reproducibility was
32 also determined using three replicate analyses of the certified reference material GBW08607.
33 This study revealed that the RSD of the Cr result was 1.87 % for GBW08607. Such results
34 indicate that FI-SCGD-AES can be employed for the quantitative determination of trace element
35 Cr in complex samples.
36
37
38
39
40
41
42
43

44 **Conclusions** 45

46 Here, we report the development of a simple, accurate Cr speciation analysis in aqueous solution
47 based on on-line-SPE and SCGD-AES. Sensitive detection of Cr (VI) was achieved with a DL of
48 $0.75 \mu\text{g}\cdot\text{L}^{-1}$, which is significantly better than an earlier study using a similar SCGD-AES
49 technique. The novel hybrid mesoporous solid selectively retained Cr (VI) with little interference
50 from Cr (III) or other cations and anions in real samples. The analytical methodology was
51 successfully applied in real water sample analyses. The certified reference material GBW08607
52 was analyzed, and the results were well consistent with the certified value.
53
54
55
56
57
58
59
60

Acknowledgements

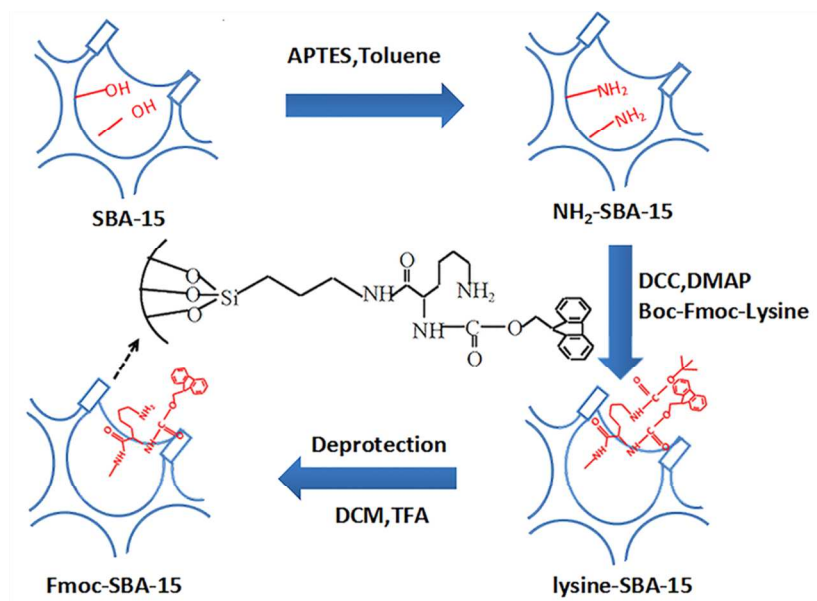
The work was financed by National Natural Science Foundation of China (No. 21175145), and the general program of the Shanghai Science and Technology Commission (No.12142200200 and No.13142201200).

1
2
3
4
5
6
7
8
9
10
11
12
13
14
15
16
17
18
19
20
21
22
23
24
25
26
27
28
29
30
31
32
33
34
35
36
37
38
39
40
41
42
43
44
45
46
47
48
49
50
51
52
53
54
55
56
57
58
59
60

References

- (1) K. S. Subramanian, *Anal. Chem.*, 1988, **60**, 11-15.
- (2) M. Sperling, S. Xu and B. Welz, *Anal. Chem.*, 1992, **64**, 3101-3108.
- (3) G. Cimino, A. Passerini and G. Toscano, *Water Res.*, 2000, **34**, 2955-2962.
- (4) D. Mohan and C. U. Pittman Jr., *J. Hazard. Mater.*, 2006, **B137**, 762-811.
- (5) X. W. Wu, H. W. Ma and Y. R. Zhang, *Appl. Clay Sci.*, 2010, **48**, 538-541.
- (6) Z. Wang, D. M. Fang, Q. Li, L. X. Zhang, R. Qian, Y. Zhu, H. Y. Qu and Y. P. Du, *Anal. Chim. Acta.*, 2012, **725**, 81-86.
- (7) O. Hazer and D. Demir, *Anal. Sci.*, 2013, **29**, 729-734.
- (8) H. F. Maltez and E. Carasek, *Talanta*, 2005, **65**, 537-542.
- (9) V. N. Bulut, C. Duran, M. Tufekci, L. Elci and M. Soylak, *J. Hazard. Mater.*, 2007, **143**, 112-117.
- (10) K. O. Saygi, M. Tuzen, M. Soylak and L. Elci, *J. Hazard. Mater.*, 2008, **153**, 1009-1014.
- (11) R. P. Monasterio, J. C. Altamirano, L. D. Martinez and R. G. Wuilloud, *Talanta*, 2009, **77**, 1290-1294.
- (12) C. R. T. Tarley, G. F. Lima, D. R. Nascimento, A. R. S. Assis, E. S. Ribeiro, K. M. Diniz, M. A. Bezerra and M. G. Segatelli, *Talanta*, 2012, **100**, 71-79.
- (13) M. L. Kim, J. D. Stipeikis and M. B. Tudino, *Talanta*, 2009, **77**, 1068-1074.
- (14) A. M. Zou, X. W. Chen, M. L. Chen and J. H. Wang, *J. Anal. At. Spectrom.*, 2008, **23**, 412-415.
- (15) A. M. Zou, X. Y. Tang, M. L. Chen and J. H. Wang, *Spectrochim. Acta, Part B.*, 2008, **63**, 607-611.
- (16) M. Kim, J. Stipeikis and M. Tudino, *Spectrochim. Acta, Part B.*, 2009, **64**, 500-505.
- (17) P. Wu, H. Chen, G. L. Cheng and X. D. Hou, *J. Anal. At. Spectrom.*, 2009, **24**, 1098-1104.
- (18) R. E. Wolf, S. A. Morman, P. L. Hageman, T. M. Hoefen and G. S. Plumlee, *Anal. Bioanal. Chem.*, 2011, **401**, 2733-2745.
- (19) B. Novotnik, T. Zuliani, A. Martinčič, J. Ščančar and R. Milačič, *J. Anal. At. Spectrom.*, 2012, **27**, 488-495.
- (20) A. J. Bednar, R. A. Kirgan and W. T. Jones, *Anal. Chim. Acta.*, 2009, **632**, 27-34.
- (21) T. Cserfalvi, P. Mezei and P. Apai, *J. Phys. D: Appl. Phys.*, 1993, **26**, 2184-2188.
- (22) P. Mezei and T. Cserfalvi, *Appl. Spectrosc. Rev.*, 2007, **42**, 573-604.
- (23) M. R. Webb and G. M. Hieftje, *Anal. Chem.*, 2009, **81**, 862-867.
- (24) P. Jamroz, K. Greda and P. Pohl, *Trends in Analytical Chemistry*, 2012, **41**, 105-121.
- (25) Q. He, Z. L. Zhu and S. H. Hu, *Appl. Spectrosc. Rev.*, 2014, **49**, 249-269.
- (26) R. Shekhar, D. Karunasagar, M. Ranjit and J. Arunachalam, *Anal. Chem.*, 2009, **81**, 8157-8166.
- (27) M. R. Webb, F. J. Andrade and G. M. Hieftje, *Anal. Chem.*, 2007, **79**, 7899-7905.
- (28) M. R. Webb, F. J. Andrade and G. M. Hieftje, *Anal. Chem.*, 2007, **79**, 7807-7812.
- (29) P. Mezei, T. Cserfalvi and L. Csillag, *J. Phys. D: Appl. Phys.*, 2005, **38**, 2804-2811.
- (30) Z. Wang, A. J. Schwartz, S. J. Ray and G. M. Hieftje, *J. Anal. At. Spectrom.*, 2013, **28**, 234-240.

- 1
2
3
4
5
6
7
8
9
10
11
12
13
14
15
16
17
18
19
20
21
22
23
24
25
26
27
28
29
30
31
32
33
34
35
36
37
38
39
40
41
42
43
44
45
46
47
48
49
50
51
52
53
54
55
56
57
58
59
60
- (31) T. A. Doroski, A. M. King, M. P. Fritz and M. R. Webb, *J. Anal. At. Spectrom.*, 2013, **28**, 1090-1095.
- (32) Y. S. Park, S. H. Ku, S. H. Hong, H. J. Kim and E. H. Piepmeier, *Spectrochim. Acta, Part B.*, 1998, **53**, 1167-1179.
- (33) H. J. Kim, J. H. Lee, M. Y. Kim, T. Cserfalvi and P. Mezei, *Spectrochim. Acta, Part B.*, 2000, **55**, 823-831.
- (34) Z. Zhang, Z. Wang, Q. Li, H. J. Zou and Y. Shi, *Talanta*, 2014, **119**, 613-619.
- (35) R. Manjusha, M. A. Reddy, R. Shekhar and S. Jaikumar, *J. Anal. At. Spectrom.*, 2013, **28**, 1932-1939.
- (36) P. G. Krishna, J. M. Gladis, U. Rambabu, T. P. Rao and G. R. K. Naidu, *Talanta*, 2004, **63**, 541-546.
- (37) O. D. Uluozlu, M. Tuzen, D. Mendil, B. Kahveci and M. Soylak, *J. Hazard. Mater.*, 2009, **172**, 395-399.
- (38) S. Sadeghi and A. Z. Moghaddam, *Talanta*, 2012, **99**, 758-766.
- (39) A. Tor, T. Büyükerkek, Y. Çengelöglu and M. Ersöz, *Desalination*, 2004, **171**, 233-241.
- (40) B. Pakzadeh and J. R. Batista, *Water Res.*, 2011, **45**, 3055-3064.
- (41) J. N. Li, L. N. Wang, T. Qi, Y. Zhou, C. H. Liu, J. L. Chu and Y. Zhang, *Microporous Mesoporous Mater.*, 2008, **110**, 442-450.
- (42) J. N. Li, T. Qi, L. N. Wang, C. H. Liu and Y. Zhang, *Mater. Lett.*, 2007, **61**, 3197-3200.
- (43) J. S. Li, X. Y. Miao, Y. X. Hao, J. Y. Zhao, X. Y. Sun and L. J. Wang, *J. Colloid Interface Sci.*, 2008, **318**, 309-314.
- (44) M. Kim, J. Stripeikis and M. Tudino, *Spectrochim. Acta, Part B.*, 2009, **64**, 500-505.
- (45) A. Shahbazi, H. Younesi and A. Badiei, *Chem. Eng. J.*, 2011, **168**, 505-518.
- (46) Z. J. Liang, B. Fadhel, C. J. Schneider and A. L. Chaffee, *Microporous Mesoporous Mater.*, 2008, **111**, 536-543.
- (47) D. Halder, *Tetrahedron*, 2008, **64**, 186-190.
- (48) S. Asuha, X. G. Zhou and S. Zhao, *J. Hazard. Mater.*, 2010, **181**, 204-210.
- (49) Z. G. Jia, K. K. Peng and L. X. Xu, *Mater. Chem. Phys.*, 2012, **136**, 512-519.
- (50) T. Chen, T. Wang, D. J. Wang, H. R. Xue, J. Q. Zhao, X. C. Ding, S. C. Wu and J. P. He, *Mater. Res. Bull.*, 2011, **46**, 1424-1430.
- (51) A. M. Yusof and N. A. N. N. Malek, *J. Hazard. Mater.*, 2009, **162**, 1019-1024.
- (52) K. Greda, P. Jamróz and P. Pohl, *Talanta*, 2013, **108**, 74-82.
- (53) Y. F. Huang, Y. Li, Y. Jiang and X. P. Yan, *J. Anal. At. Spectrom.*, 2010, **25**, 1467-1474.



Scheme 1. Synthetic route for Fmoc-SBA-15.

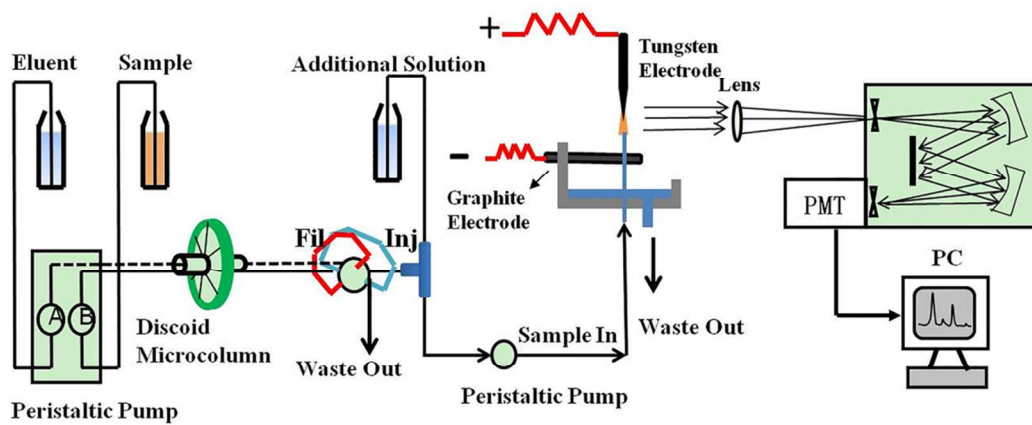


Figure 1. Schematic diagram of FI-SCGD-AES system.

Table 1. Operation sequence of the FI-SCGD-AES for Cr (VI) determination.

| Step | Pump | Delivered medium | Flow rate (mL·min ⁻¹) | Time (s) | Valve | Function |
|------|------|---------------------|-----------------------------------|----------|--------|----------------|
| 1 | A | Sample | 4 | 420 | Inject | Extraction |
| | B | eluent ^a | 1.5 | 420 | | |
| 2 | A | Sample | 0 | 0 | Fill | Elution |
| | B | eluent ^a | 1.5 | 120 | | |
| 3 | A | Water | 4 | 60 | Inject | Washing system |
| | B | eluent ^a | 0 | 0 | | |

^aeluent was 0.1 mol·L⁻¹ NH₃·H₂O.

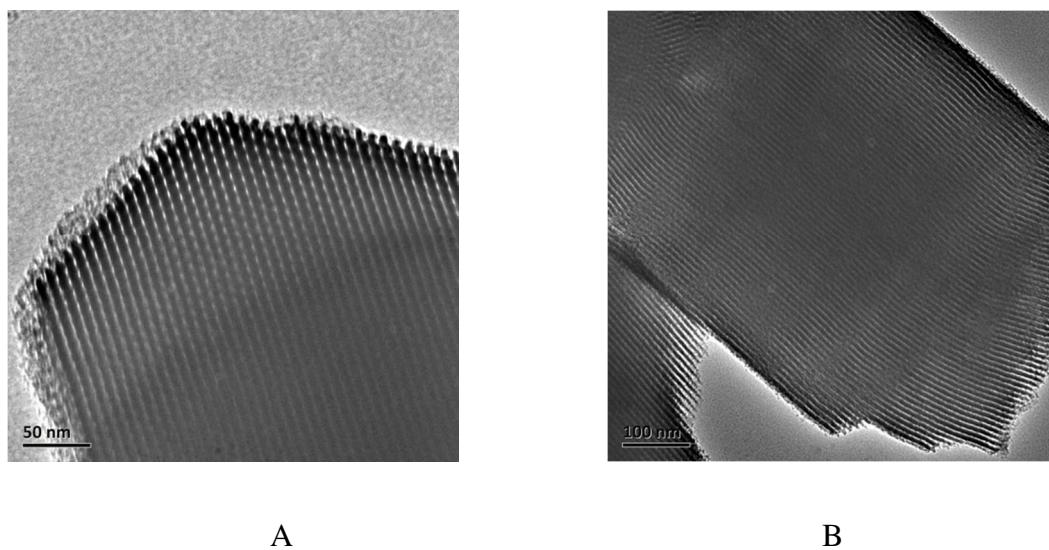


Figure 2. TEM images of Fmoc-SBA-15 with electron beams parallel (A) and perpendicular (B) to the pore channels.

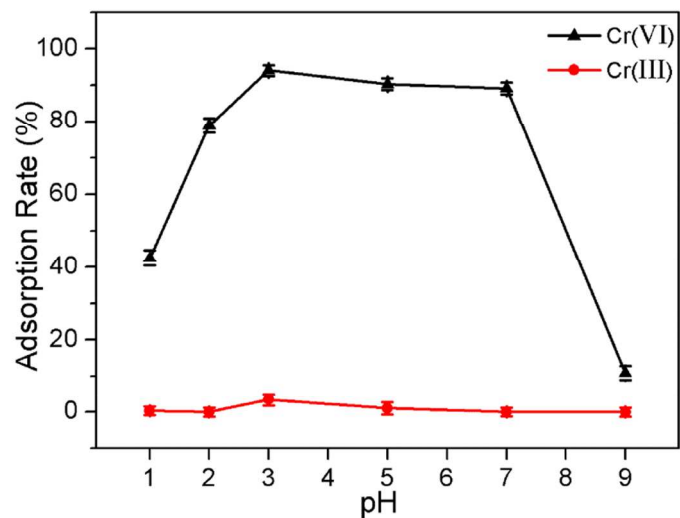


Figure 3. Influence of initial pH on Cr (VI) and Cr (III) adsorption ($10 \text{ mg}\cdot\text{L}^{-1}$; adsorbent dose = $1 \text{ g}\cdot\text{L}^{-1}$; 60 min).

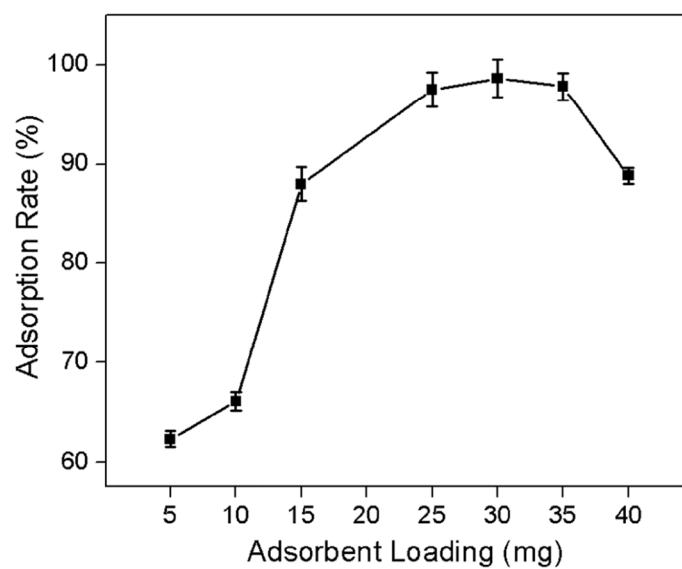


Figure 4. Effect of the mesoporous material loading on the adsorption rate of Cr (VI).

Table 2. Influence of coexisting ions on the determination of 100 $\mu\text{g}\cdot\text{L}^{-1}$ Cr (VI).

| Coexisting ion | Concentration ($\mu\text{g}\cdot\text{L}^{-1}$) | Recovery (%) | Coexisting ion | Concentration ($\mu\text{g}\cdot\text{L}^{-1}$) | Recovery (%) |
|----------------|---|--------------|---------------------------|---|--------------|
| Pb(II) | 1000 | 102 | Cr(III) | 500 | 99 |
| Ca(II) | 5000 | 87 | Cl^- | 50000 | 102 |
| Mg(II) | 4000 | 100 | H_2PO_4^- | 100000 | 93 |
| Zn(II) | 5000 | 88 | SO_4^{2-} | 20000 | 86 |
| Al(III) | 4000 | 94 | NO_3^- | 50000 | 92 |

Table 3. Analytical performance of the present SCGD-AES for Cr determination compared with other SCGD-AES.

| Detection technique | Detection Limits (DLs, $\mu\text{g}\cdot\text{L}^{-1}$, Cr, 357.9 nm) | The method of increasing sensitivity |
|---------------------------|--|--------------------------------------|
| ELCAD-AES ³² | 900.0 | / |
| dc-APGD-AES ⁵² | 400.0 | / |
| ELCAD-AES ³³ | 200.0 | / |
| ELCAD-AES ³⁴ | 65.0 | Enhancement using HCOOH |
| SCGD-AES ³⁵ | 42.0 | Enhancement using CTAC |
| Present Work | 0.75 | SPE preconcentration |

Table 4. Comparison of the analytical features of merit of this and other methods for Cr determination based on on-line SPE coupled with atomic spectrometry or ICP-MS.

| Adsorbent | Analyte | Detection technique | EF ^a | LOD ^b ($\mu\text{g}\cdot\text{L}^{-1}$) | RSD ^c (%) | Linearity range ($\mu\text{g}\cdot\text{L}^{-1}$) | Reference |
|--|---------|---------------------|-----------------|---|-------------------------|--|-----------|
| Fmoc-SBA-15 | Cr(VI) | SCGD-AES | 91 | 0.75 | 4.2 | 10–10000 | This work |
| NH ₂ -SBA-15 | Cr(VI) | FAAS | 44.0 | 0.2 | 2.1 | 10–100 | [6] |
| Resin | Cr(VI) | FAAS | 30 | 2.4 | 3.0 | – | [7] |
| Modified silica gel | Cr(VI) | FAAS | 24.9 | 2.3 | 2.1 | 25–250 | [8] |
| | Cr(III) | | 20.8 | 1.9 | 3.0 | 25–250 | |
| Amberlite XAD-2010 resin | Cr(VI) | FAAS | 25 | 1.28 | <5 | - | [9] |
| Dowex M4195 chelating | Cr(VI) | FAAS | - | 1.94 | <10 | - | [10] |
| Animal fiber | Cr(VI) | FAAS | 32 | 0.3 | 4.3 | - | [11] |
| | | | 17.6 | 0.66 | 2.4 | | |
| | | | 2 | | | | |
| SiO ₂ /Al ₂ O ₃ /TiO ₂ | Cr(III) | FAAS | 32.9 | 0.27 | 6.4 | 10–375 | [12] |
| | Cr(VI) | | 8 | | | | |
| Hybrid mesoporous materials | Cr(VI) | ETAAS | 16.0 | 0.09 | 1.8 | 0.09–3 | [13] |
| Egg-shell membrane | Cr(VI) | ETAAS | 13.3 | 0.01 | 3.2 | 0.05–1.25 | [14] |
| 717 anion exchange resin | Cr(VI) | ETAAS | 11.6 | 0.03 | 2.5 | 0.12–0.2 | [15] |
| | Cr(III) | | 10.5 | 0.02 | 1.9 | 0.1–0.25 | |
| A hybrid mesoporous solid | Cr(VI) | ETAAS | 27 | 0.0012 | 2.5 | 0.004–0.5 | [16] |
| Nano-TiO ₂ | Cr(VI) | ETAAS | 3.6 | 0.01 | 1 | - | [17] |
| | Cr(III) | | 4.8 | 0.006 | 0.5 | | |
| magnetic microspheres | Cr(VI) | ICP-MS | 47 | 0.0015 | 4.5 | - | [53] |
| | Cr(III) | | 96 | 0.0021 | 1.9 | | |

^aEnrichment factor.^bLimit of detection.^cPrecision.

Table 5. Cr determination in DIW and wastewater using the proposed method.

| Sample | Cr(VI) added ($\mu\text{g}\cdot\text{L}^{-1}$) | Cr(III) added ($\mu\text{g}\cdot\text{L}^{-1}$) | Cr(VI) determined ($\mu\text{g}\cdot\text{L}^{-1}$) | Cr(III) determined ($\mu\text{g}\cdot\text{L}^{-1}$) | Cr(VI) recovery (%) |
|----------------|--|---|---|--|---------------------------|
| DIW | 0 | 0 | Not found | Not found | - |
| | 50.0 | 0 | 51.2 \pm 1.6 | 0 | 102 |
| Waste water | 0 | 0 | Not found | Not found | - |
| | 40.0 | 100.0 | 39.5 \pm 1.2 | 101.2 \pm 1.4 | 99 |
| | 60.0 | 100.0 | 60.6 \pm 0.9 | 100.3 \pm 2.6 | 101 |

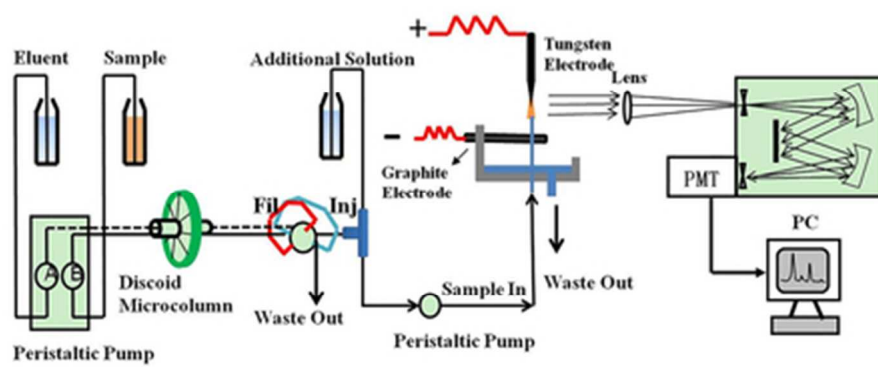


Figure 1. Schematic diagram of FI-SCGD-AES system.
37x17mm (300 x 300 DPI)

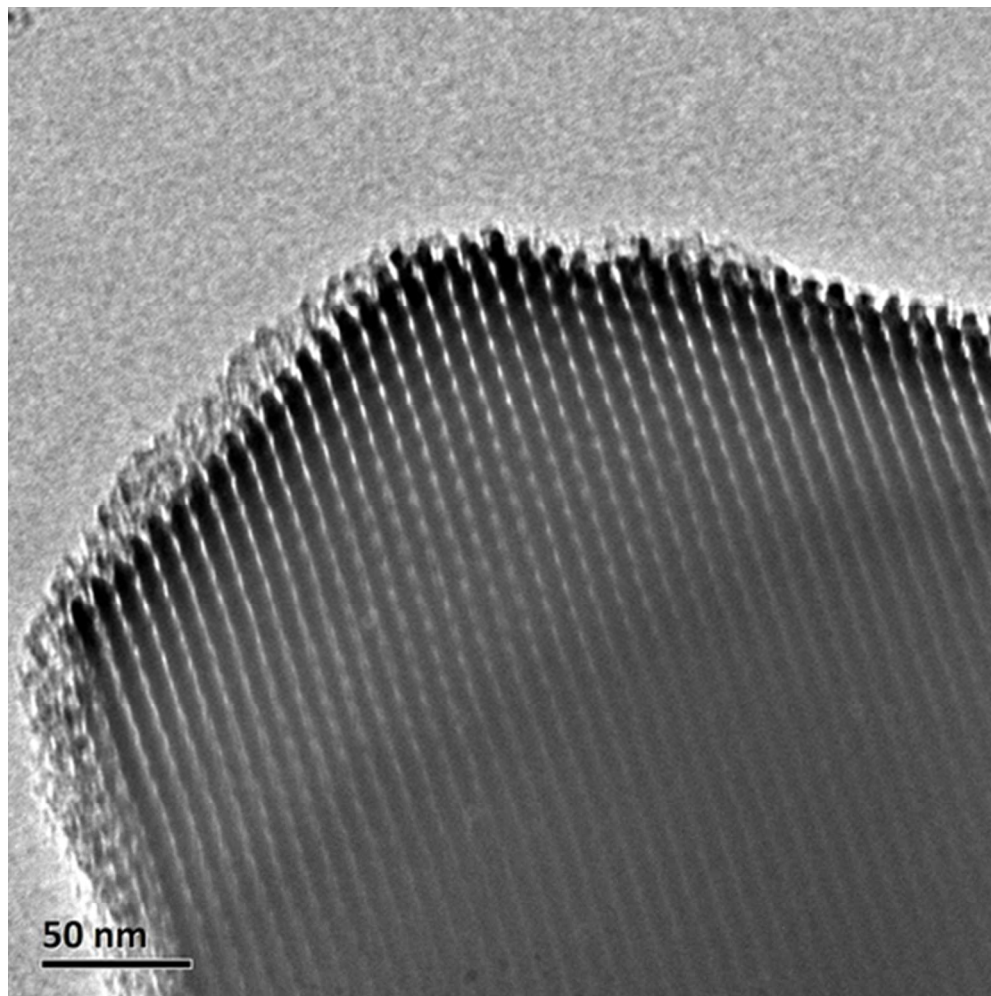


Figure 2A. TEM images of Fmoc-SBA-15 with electron beams parallel to the pore channels.
41x41mm (300 x 300 DPI)

1
2
3
4
5
6
7
8
9
10
11
12
13
14
15
16
17
18
19
20
21
22
23
24
25
26
27
28
29
30
31
32
33
34
35
36
37
38
39
40
41
42
43
44
45
46
47
48
49
50
51
52
53
54
55
56
57
58
59
60

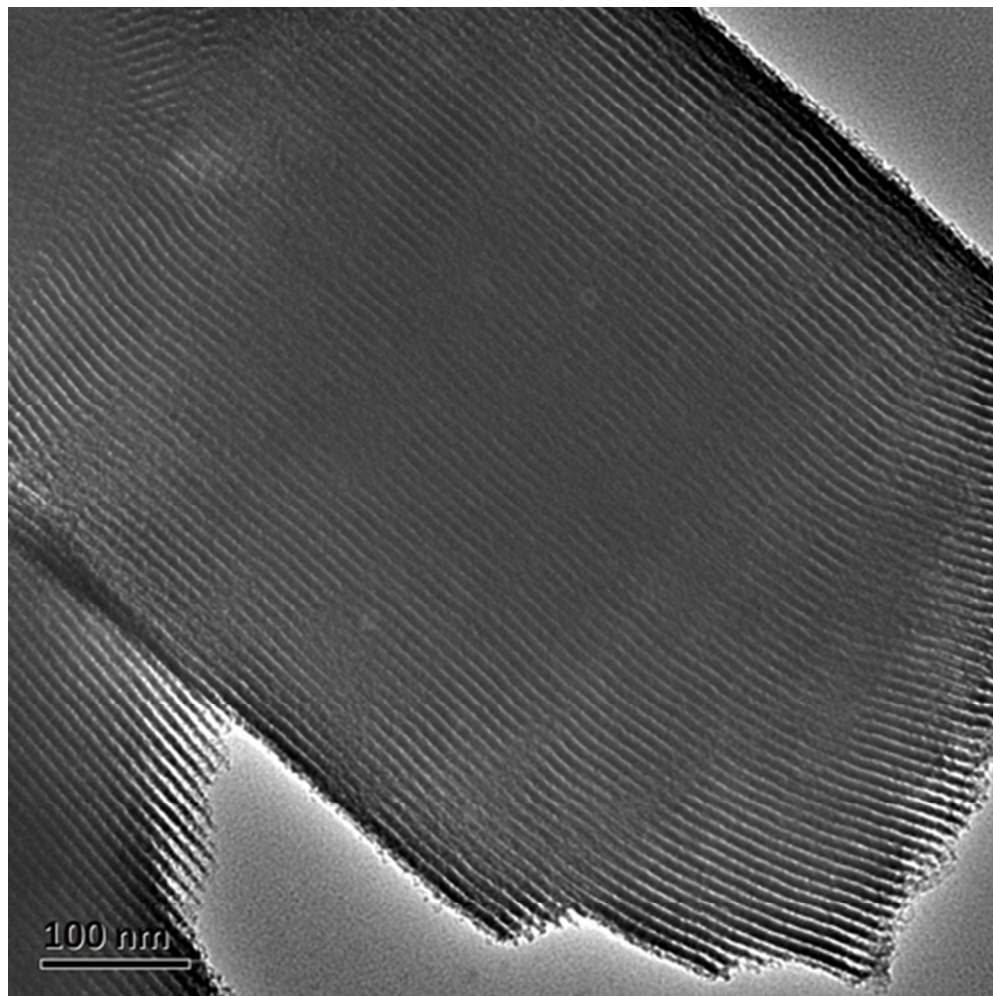


Figure 2B. TEM images of Fmoc-SBA-15 with electron beams perpendicular to the pore channels.
41x41mm (300 x 300 DPI)

1
2
3
4
5
6
7
8
9
10
11
12
13
14
15
16
17
18
19
20
21
22
23
24
25
26
27
28
29
30
31
32
33
34
35
36
37
38
39
40
41
42
43
44
45
46
47
48
49
50
51
52
53
54
55
56
57
58
59
60

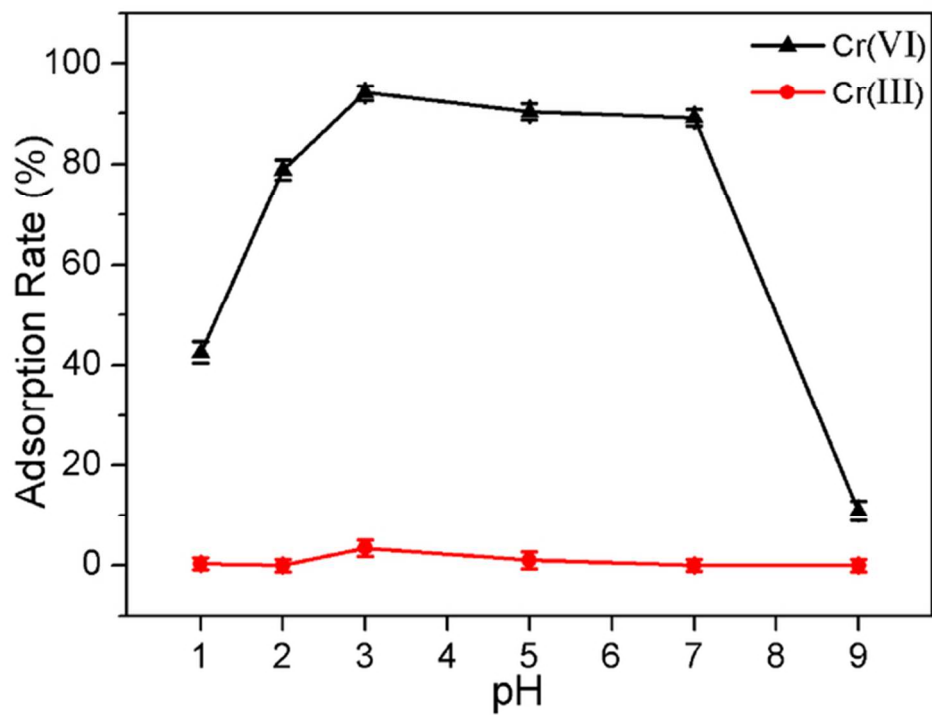


Figure 3. Influence of initial pH on Cr (VI) and Cr (III) adsorption ($10 \text{ mg}\cdot\text{L}^{-1}$; adsorbent dose = $1 \text{ g}\cdot\text{L}^{-1}$; 60 min).
61x46mm (300 x 300 DPI)

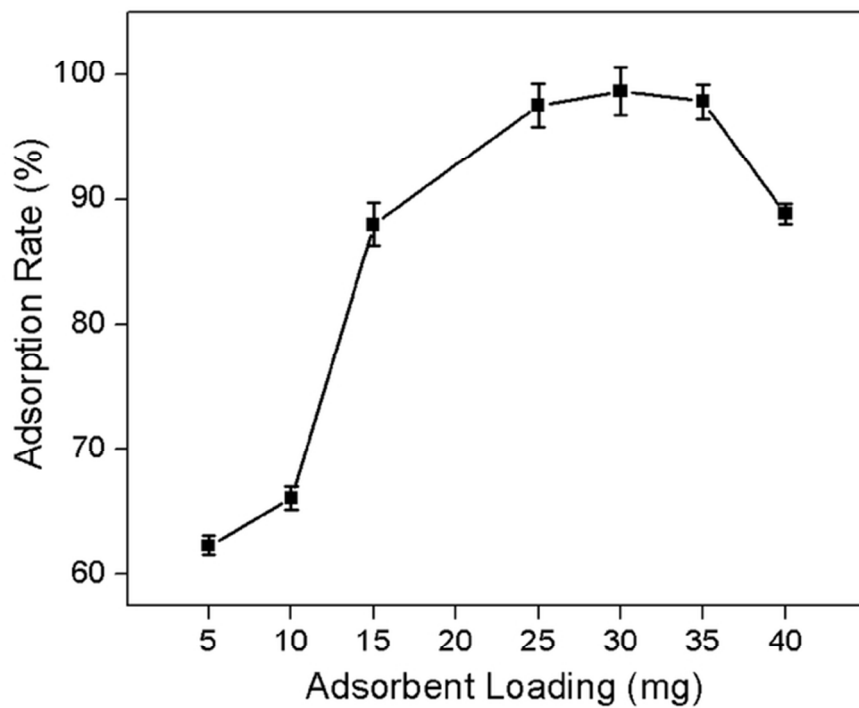
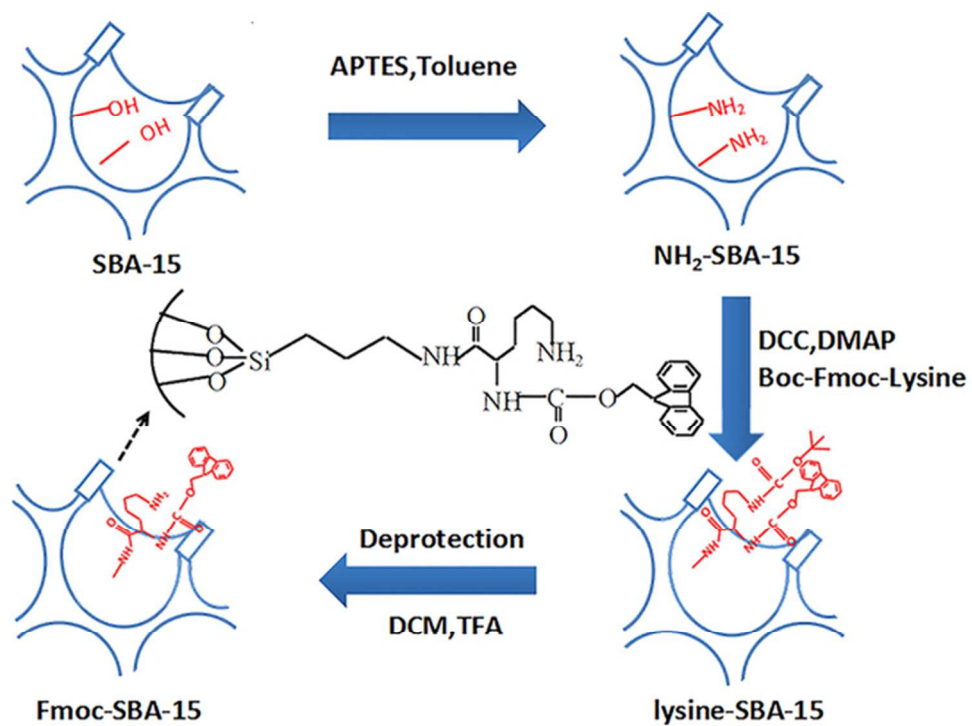


Figure 4. Effect of the mesoporous material loading on the adsorption rate of Cr (VI).
63x49mm (300 x 300 DPI)



Scheme 1. Synthetic route for Fmoc-SBA-15.
57x41mm (300 x 300 DPI)